한국계산과학공학회

2026년 추계학술발표대회

2026 Fall Conference of Korean Society for Computational Sciences and Engineering

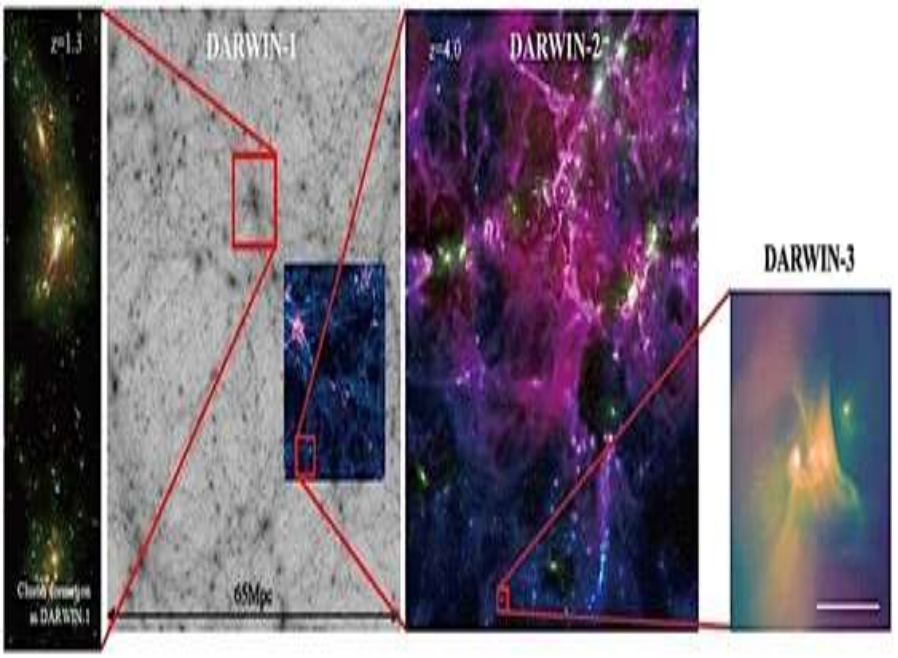

한국계산과학공학회
Korean Society for Computational Sciences and Engineering

목 차

학술대회 프로그램

시 간	발표 논문	발표자(소속)
13:30~13:40	**환영 인사 및 축사**	김종수 (회장)
1부	**좌장 : 김종수 회장**	
13:40~14:05	Simulating the Formation and Evolution of Dwarf Galaxies on a Next-Generation National Supercomputer	김용휘 (KISTI)
14:05~14:30	Effects of Rain-Gauge Network Variability on CycleGAN-Based Precipitation Estimation	김효진 (KISTI)
14:30~14:55	Fichera-corner First-passage Algorithm	이재호 (GIST)
14:55~15:20	Artificial Intelligence-Fokker-Planck Equation Hybrid for Optimal Descriptor Identification and Prognosis of Patient Fate Dynamics	정인춘 (중앙대학교)
15:20~15:50	**Break Time / 포스터 관람**	
2부	**좌장 : 이영민 수석 부회장**	
15:50~16:15	Test Vector Generator for the ALMA Wideband Sensitivity Upgrade: Application of NVIDIA DOCA GPUNetIO	김종수 (KASI)
16:15~16:40	Size-dependent free energy of micelles extracted from their size distribution and development of novel, efficient free energy calculation method	박진원 (중앙대학교)
16:40~17:05	Toward Multimodal AI for Drug Discovery: From ADMET Prediction and Molecular Generation to Foundation Models	한혜림 (나무ICT)
17:05~17:30	Q-CAR: A Noise and Congestion-Aware Deployment Scheme for Quantum Job Scheduling on Slurm Clusters	하지원 (서울대학교)
(*) 포스터 논문		
DeepKinomeWeb: a Quantitative, Panel-Level Platform for Kinase Inhibitor Screening and Selectivity Profiling		나현수 (KRIBB)
pH-dependent membrane insertion and folding of the Caveolin-3-derived peptide Cav3(7-26): an all-atom molecular dynamics study		양승훈 (KRIBB)
Virtual Screening of Covalent Inhibitors Targeting PNPLA3-I148M		김애진 (KRIBB)
Computational modeling of the AAVX-AAVR complex from Cryo-EM density map		전홍욱 (KRIBB)

Simulating the Formation and Evolution of Dwarf Galaxies on a Next-Generation National Supercomputer

Yonghwi Kim[1*], and DARWIN Collaboration

[1] *Korea Institute of Science and Technology Information (KISTI), Daejeon 34141, Republic of Korea*

Corresponding author (Electronic mail: yonghwi.kim@kisti.re.kr)

Dwarf galaxies present a profound challenge for numerical simulations. Their shallow potential wells are highly susceptible to stellar feedback, necessitating that kiloparsec-scale outcomes be modeled alongside parsec-scale physics. Bridging this gap requires a spatial dynamic range of six orders of magnitude— a major computational and astrophysical challenge. This effort is timely, as dwarf galaxies are a primary observational target for upcoming next-generation telescopes.

We report the status of DARWIN (DAzzling Realization of dWarf galaxies In the Next generation), a 3-step cosmological simulation campaign achieving this dynamic range via nested refinement. The framework couples adaptive mesh refinement hydrodynamics with particle-mesh gravity, multi-band radiative transfer, and stiff thermochemical networks tracking over 12 species. Thus, computational costs are dominated by operator coupling and load imbalances inherent to this multi-physics system. DARWIN-1 evolves a 65 Mpc volume at 0.5 kpc, reproducing observed scaling relations across stellar mass, halo mass, chemical abundances, and central black hole mass. In DARWIN-2, 24 sub-regions were resimulated at 62.5–125 pc, yielding 243 dwarf galaxies and demonstrating environmental regulation on gas accretion: chemically pristine systems decrease tenfold near massive neighbors. DARWIN-3 reaches a 3.9 pc resolution across 16 zoom-in targets, resolving early star formation and gas stripping.

Since each stage incurs a computational cost 500 times greater than its predecessor, standard CPU-only architectures cannot sustain this scaling. Future progress necessitates utilizing the KISTI-6 national flagship supercomputer, HANGANG, and its accelerated solver, serving as the primary motivation for the numerical work presented separately at this conference.

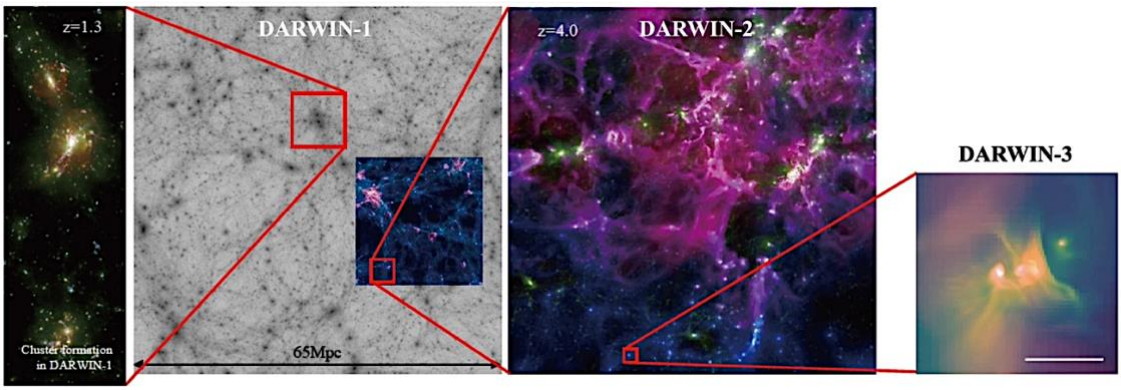

Figure 1 3-Steps of DARWIN Simulations

Acknowledgments This research is supported by the National Research Foundation of Korea (NRF) grant funded by the Korea government (MIST) (No. 2022M3K3A1097104). This work is also supported by KISTI under the institutional R&D project (K26L1M2C3).

References

[1] Ahn, J., Kim, W.-T., & Kim, Y., ApJS, 280, 35 (2025).

[2] DARWIN Collaboration, ApJ (2026, submitted)

[3] KISTI Official Announcement, KISTI Expands AI and HPC Collaboration with NVIDIA and HPE Based on Supercomputer No. 6 “HANGANG” (2026).

Effects of Rain-Gauge Network Variability on CycleGAN-Based Precipitation Estimation

Hyojin Kim [1*], Wonsu Kim[1]

[1] *Korea Institute of Science and Technology Information, Daejeon 34141, Republic of Korea*

Corresponding author (Electronic mail: hjkim@kisti.re.kr)

Accurate reconstruction of spatial rainfall patterns from sparsely distributed ground observations remains challenging. To address this problem, a CycleGAN-based approach was developed to learn spatial precipitation characteristics from radar data while retaining rainfall information observed at rain gauges. The effects of changes in the available gauge network were further investigated by evaluating model performance under varying rain-gauge network configurations. Rain-gauge precipitation and a station-location mask were used as inputs. The model generally achieved higher CSI values than radar and IMERG at gauges excluded from the input. Model performance deteriorated as the number of input gauges decreased below that used during training, particularly for intense precipitation. To improve applicability to different observation environments, diverse gauge configurations were incorporated during training. This strategy reduced performance degradation in a new region with a sparse gauge network and achieved performance comparable to a model trained directly on the target region. These results suggest that considering diverse gauge-network configurations during model training is important for practical application.

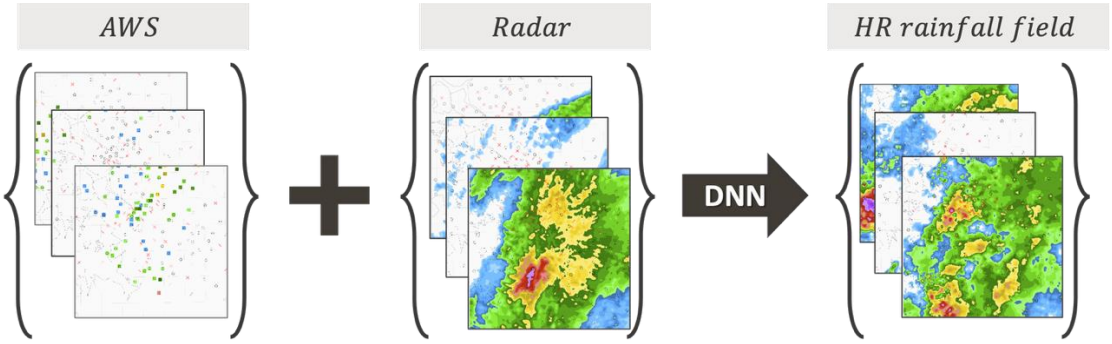

Figure 1 Schematic of high-resolution rainfall field generation from AWS and radar data

Acknowledgments This work was supported by the Korea Institute of Science and Technology Information (K26L4M1C1).

References

[1] J.-Y. Zhu et al., “Unpaired Image-to-Image Translation Using Cycle-Consistent Adversarial Networks,” ICCV, 2223-2232 (2017).
[2] H. Wernli et al., “Sal a novel quality measure for the verification of quantitative precipitation forecasts,” Monthly Weather Review, 136, 4470–4487, (2008).
[3] G. Ma et al., “An improved deep-learning-based precipitation estimation algorithm using multitemporal goes-16 images,” IEEE Transactions on Geoscience and Remote Sensing, 62, (2024).
[4] R. Sarafian al., “RadarGaugeNet: Radar-rain-gauge-based ai architecture for real-time quantitative precipitation estimation,” IEEE Transactions on Geoscience and Remote Sensing, 63, (2025).

Fichera-corner First-passage Algorithm

Jae-ho Lee[2], Sungwon Cho[3], Geonho Hwang[1*], and Chi-Ok Hwang[1†]

[1]Department of Mathematical Sciences, College of Natural Sciences,

Gwangju Institute of Science and Technology,

Gwangju Metropolitan City 61005, South Korea

[2]Department of Physics and Photon Science, College of Natural Sciences,

Gwangju Institute of Science and Technology,

Gwangju Metropolitan City 61005, South Korea and

[3]Department of Electrical Engineering and Computer Science,

College of Artificial Intelligence, Gwangju Institute of Science and Technology,

Gwangju Metropolitan City 61005, South Korea

[*]Corresponding author (E-mail address: hgh2134@gist.ac.kr)

[†]Corresponding author(E-mail address: chwang@gist.ac.kr)

In Diffusion Monte Carlo simulations, the “Walk-on-Spheres” (WOS) algorithm requires an absorption ϵ-layer to terminate diffusion near boundaries, inevitably inducing artificial truncation errors. This inefficiency is especially magnified near complex geometries like edges and corners. Exploiting the electrostatic-diffusion isomorphism, exact boundary-specific algorithms like Walk- on-Plane and Walk-on-Infinite-L-shaped (WOIL) have been developed. Extending this approach, we introduce a novel Walk-on-Infinite-Fichera-Corner (WOIFC) first-passage algorithm. By deriv- ing the exact first-passage probability distribution on an infinite Fichera-corner (cubic trihedral) boundary, we developed an acceptance-rejection sampling method for exact random walk jumps. To demonstrate this, an application combining WOIFC with WOS and WOIL to sample first-passage collision points within a finite cube is currently in progress.

Keywords: Monte Carlo, First-passage, Fichera-corner, Acceptance-rejection sampling

Artificial Intelligence-Fokker-Planck Equation Hybrid for Optimal Descriptor Identification and Prognosis of Patient Fate Dynamics

In-Chun Jeong[a,b,c], Ji-Hyun Kim[a,b,c,*], Jaeyoung Sung[a,b,c,*]

[a]Global Science Research Center for Systems Chemistry, Chung-Ang University; Seoul 06974, Republic of Korea.
[b]Creative Research Initiative Center for Chemical Dynamics in Living Cells, Chung-Ang University; Seoul 06974, Republic of Korea.
[c]Department of Chemistry, Chung-Ang University; Seoul 06974, Republic of Korea.
**Correspondence should be addressed to jihyunkim@cau.ac.kr (J.-H. Kim) and jaeyoung@cau.ac.kr (J.S.).*

Sepsis is a life-threatening critical illness that poses formidable clinical challenges. Its abrupt onset and heterogeneous pathophysiology impede early diagnosis and timely therapeutic intervention. In the absence of a gold standard for early sepsis diagnosis, deep learning (DL) approaches have been widely explored for both diagnosis and prognosis; however, a unified artificial intelligence (AI) framework that delivers accurate diagnostic and prognostic predictions for sepsis patients remains lacking. In this talk, we introduce an artificial intelligence-Fokker-Planck Equation (AI-FPE) hybrid framework for the construction of an effective descriptor characterizing a patient's clinical state and the prediction of clinical outcomes based on the probabilistic dynamics of this descriptor. From the AI module of this framework, we derive the Septic Infection-Related Risk Index (SIRRI), an interpretable descriptor that effectively represents the pathological severity of sepsis patients. The Fokker-Planck Equation-based prognostic module further predicts the temporal evolution of SIRRI distributions, time-dependent mortality and recovery rates across different clinical stages. Improving this framework, we are currently developing AI-based multidimensional representations of patient state, where distinct dimensions encode complementary aspects of the pathological state and disease progression of patients. This project requires systematic exploration of large-scale clinical datasets and diverse model architectures, integration with transcriptome analyses to establish biological relevance, and rigorous validation across independent external cohorts.

Test Vector Generator for the ALMA Wideband Sensitivity Upgrade: Application of NVIDIA DOCA GPUNetIO

Jongsoo Kim
Korea Astronomy and Space Science Institute

The Atacama Large Millimeter/submillimeter Array (ALMA) is undergoing its Wideband Sensitivity Upgrade (WSU) to significantly enhance its scientific observing capabilities. In the upgraded system, each antenna produces four high-speed digital data streams. Digitized at an ultra-high rate of 40 Giga-samples per second with 6-bit resolution, each stream generates a payload data rate of 240 Gbps (40 GSPS x 6 bits/sample), totaling nearly 1 Tbps per antenna. Developing and validating the downstream GPU-based real-time processing pipelines requires realistic input signal streams; however, relying on physical telescope digitizers or dedicated hardware fixtures during development is inflexible and cost-prohibitive.

To solve this challenge, we developed the Test Vector Generator (TVG)—an autonomous, software-defined signal generation system implemented on the NVIDIA GH200 Grace Hopper Superchip using NVIDIA DOCA GPUNetIO. TVG synthesizes realistic astronomical noise signals, encapsulates standard network packets directly within GPU High Bandwidth Memory, and streams them over 400 Gbps Ethernet links with zero host CPU involvement. By leveraging GPU-initiated transmission and hardware burst pacing on the NVIDIA ConnectX-7 network adapter, the system eliminates operating system jitter and delivers deterministic, line-rate packet streaming with nanosecond precision.

Benchmarking on the GH200 demonstrates that TVG achieves sustained generation and transmission speeds exceeding 270 Gbps per stream (accounting for protocol overhead) with substantial real-time safety margins. TVG provides a versatile, cost-effective test platform that successfully verifies high-throughput astronomical signal processing pipelines without specialized hardware.

Size-dependent free energy of micelles extracted from their size distribution and development of novel, efficient free energy calculation method

jinwon Park[1,2], Minho Lee[1,2], Donghee Kim[1,2], Ji-Hyun Kim[1,2] and Jaeyoung Sung[1,2]*

[1]Department of Chemistry, Chung-Ang University, Seoul, 06974, Republic of Korea
[2]Creative Research Initiative Center for Chemical Dynamics in Living Cells, 06974 Seoul, Republic of Korea

Micelles are widely used as membrane-mimetic systems for structural and functional studies of membrane proteins [1]. Micellar assemblies have also been extensively investigated as carriers for therapeutic drugs. As their size can significantly affect drug accumulation, tissue penetration, and therapeutic efficacy [2], understanding and controlling the micelle size distribution is important for both fundamental studies and practical applications. Recently, a statistical-thermodynamic theory for mesoscopic nucleation systems was developed, which successfully explains the equilibrium size distributions of nanoparticles and biological condensates [3]. However, corresponding understanding and prediction of the micelle size distribution have yet to be achieved for lack of accurate information about the size-dependent free energy of micelles. In this talk, we will introduce a new method to extract the size-dependent free energy and chemical potentials of micelles from the experiments or large-scale simulation results for the equilibrium size distribution of micelles. Time permitted, we will also talk about an alternative free energy calculation method that is free of the charging process and far more efficient than the thermodynamic integration or free energy perturbation methods.

Reference

[1] M. Das, Y. Du, J. S. Mortensen, M. Ramos, L. Ghani, H. J. Lee, H. E. Bae, B. Byrne, L. Guan, C. J. Loland, B. K. Kobilka, and P. S. Chae, “Trehalose-cored amphiphiles for membrane protein stabilization: importance of the detergent micelle size in GPCR stability,” *Organic & Biomolecular Chemistry*, **17**, 3249–3257 (2019).

[2] J. Wang, W. Mao, L. L. Lock, J. Tang, M. Sui, W. Sun, H. Cui, D. Xu, and Y. Shen, “The Role of Micelle Size in Tumor Accumulation, Penetration, and Treatment,” *ACS Nano*, **9**, 7195–7206 (2015).

[3] J. Kang, D. Kim, S. Song, J. Han, Y. Jung, S. Yoon, Y. Ryu, S. Kim, B. H. Kim, J.-M. Choi, M. Yang, J. Jang, T. Hyeon, J. Park, J.-H. Kim, and J. Sung, “Supersaturation, Nucleation, and Phase Separation of Mesoscopic Systems,” *Journal of the American Chemical Society*, **147**, 46976–46985 (2025).

Toward Multimodal AI for Drug Discovery: From ADMET Prediction and Molecular Generation to Foundation Models

Herim Han[1], Sunghwan Choi[2], Jin Hee Lee[1], and Min Sun Yeom[1*]

[1]*NamuICT R&D Center, NamuICT, 41 Magok Jungang 8-ro, Seoul 07793, Republic of Korea*

[2]*Department of Chemistry, Inha University, 100 Inha-ro, Michuhol-gu, Incheon 22212, Republic of Korea*

Corresponding author (Electronic mail: ms.yeom@namuict.co.kr)

Artificial intelligence has been increasingly applied across various stages of drug discovery, from molecular property prediction to de novo molecular generation. Among these applications, accurate prediction of ADMET properties directly from molecular structures has remained a major challenge in drug discovery. To address this challenge, we developed a AutoML-based predictive models for 11 ADMET endpoints using SMILES-derived molecular descriptors and fingerprints [1]. Automated optimization of algorithms and hyperparameters achieved AUC values above 0.80 across all endpoints, with model generalizability further evaluated through cross-validation and external validation. Beyond property prediction, we explored molecular generation with an improved molecular representation [2]. Although SMILES is a widely used and general representation of chemical structures, its atom-level representation has limitations in distinguishing identical atoms in different chemical environments. To address this limitation, a hybrid SMILES and atom-in-SMILES (AIS) representation was introduced to incorporate local atomic environment information. This representation improves token diversity and reduces token imbalance, providing a more informative representation for molecular generation. Extending these efforts, we introduce a new multimodal foundation model that aligns three complementary molecular views—SMILES, property, and distance features—through contrastive learning, enabling its application to diverse downstream tasks.

Acknowledgments This work has been carried under the support of Korean Society for Computational Science and Engineering and Korea Institute of Science and Technology Information (KISTI).

References

[1] Han H, Shaker B, Lee JH, et al (2025) Employing Automated Machine Learning (AutoML) Methods to Facilitate the *In Silico* ADMET Properties Prediction. J Chem Inf Model 65:3215–3225. https://doi.org/10.1021/acs.jcim.4c02122

[2] Han H, Yeom MS, Choi S (2025) Hybridization of SMILES and chemical-environment-aware tokens to improve performance of molecular structure generation. Sci Rep 15:16892. https://doi.org/10.1038/s41598-025-01890-7

Q-CAR: A Noise and Congestion-Aware Deployment Scheme for Quantum Job Scheduling on Slurm Clusters

Jiwon Ha[†1], Sookyoung Park[†2], Hyeonsang Eom[1], and Yoonhee Kim[2*]

1 Seoul National University, South Korea ({jwh0245,hseom}@snu.ac.kr)

2 Sookmyung Women's University, South Korea ({blue,yulan}@sookmyung.ac.kr)

† Contributed equally. * Corresponding author (Electronic mail: yulan@sookmyung.ac.kr)

NISQ-era quantum computing increasingly requires resource managers to schedule jobs across heterogeneous backends with different noise levels and queue conditions. Although noise-aware placement can improve execution fidelity by assigning sensitive circuits to low-noise devices, concentrating many such jobs on a premium backend can create severe queueing and increase overall makespan. This work presents Q-CAR (Congestion-Aware Quantum Resource Allocation), a lightweight adaptive scheduling policy for Slurm-managed heterogeneous quantum clusters. Q-CAR follows a three-stage approach: it first restricts each job to a candidate set according to per-instance noise sensitivity, then selects a node by minimizing a composite cost that combines expected waiting time, service time, and fidelity loss, and finally allows a one-tier escape when congestion on the premium node exceeds a threshold. We evaluate Q-CAR on a real Slurm resource-management layer with per-node Qiskit Aer GPU simulators configured with three controlled noise tiers. The workload consists of five MQT Bench circuit families over 2-16 qubits, and congestion is varied by changing the density of noise-sensitive jobs. Compared with a fidelity-aware baseline that sends all high- and medium-sensitivity jobs to the lowest-noise node, Q-CAR reduces makespan by 49% and 60% at 50% and 75% noise-sensitive job density, respectively, while limiting the loss in noise-sensitive fidelity to approximately 0.04-0.05. The throughput advantage remains consistent under different arrival patterns. These results show that separating fidelity-oriented candidate gating from congestion-aware allocation is an effective way to balance fidelity and throughput in the evaluated heterogeneous quantum-cluster environment.

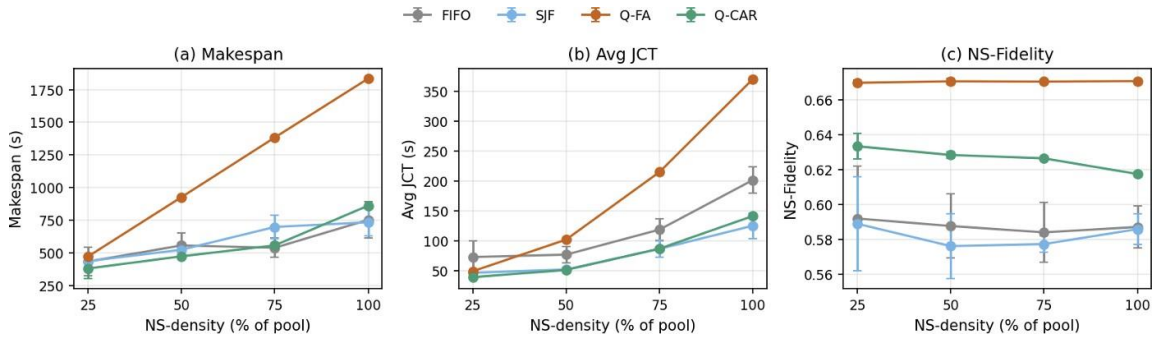

Acknowledgments This work was supported by the National Research Foundation of Korea (NRF) grant funded by the Korea government (MSIT) (No. RS-2025-24534879) and by BK21 FOUR Intelligence Computing (Dept. of Computer Science and Engineering, SNU) funded by the National Research Foundation of Korea (NRF) (4199990214639).

References

[1] A. B. Yoo, M. A. Jette, and M. Grondona, "SLURM: Simple Linux Utility for Resource Management," JSSPP, pp. 44-60 (2003).

[2] N. Quetschlich, L. Burgholzer, and R. Wille, "MQT Bench: Benchmarking Software and Design Automation Tools for Quantum Computing," Quantum, 7, 1062 (2023).

DeepKinomeWeb: a Quantitative, Panel-Level Platform for Kinase Inhibitor Screening and Selectivity Profiling

Hyeonsu Na[1,2], Jisu Eun[1,3], Yeeun Lee[4], Seunghoon Yang[1,2], Donghwan Choi[1], Hyeyun Cho[1,2], Seungyoon Nam[4,5*], and Jinhyuk Lee[1,2*]

[1] *Bio-design Editing Research Center, Korea Research Institute of Bioscience and Biotechnology (KRIBB), Daejeon 34141, Republic of Korea*

[2] *Department of Bioinformatics, KRIBB School of Bioscience, University of Science and Technology (UST), Daejeon 34141, Republic of Korea*

[3] *MolCube, Inc., 3F IT Tower, 43 Hyoryeong-ro, Seocho-gu, Seoul 06694, Republic of Korea*

[4] *Department of Genome Medicine and Science, Gachon Institute of Genome Medicine and Science, Gachon University Gil Medical Center, Gachon University College of Medicine, Incheon 21565, Republic of Korea*

[5] *Department of Health Sciences and Technology, Gachon Advanced Institute for Health Sciences and Technology (GAIHST), Gachon University, Incheon 21999, Republic of Korea*

Corresponding authors (Electronic mail: nams@gachon.ac.kr; jinhyuk@kribb.re.kr)

Protein kinases constitute one of the largest enzyme families in the human genome and remain among the most important therapeutic target classes in oncology [1, 2]. In early-stage drug discovery, however, identifying potent and selective inhibitors is constrained by the cost of competition-based high-throughput screening and by the difficulty of reading selectivity across an entire kinase panel rather than kinase by kinase. Few available tools combine panel-level screening, quantitative affinity estimation, and off-target assessment in a single workflow.

To address this gap, we developed DeepKinomeWeb, an integrated web platform for quantitative kinase inhibitor screening and selectivity profiling [4]. It builds on DeepKinome, a 20-layer convolutional neural network regression model trained on LINCS KINOMEscan data that predicts binding affinity as a continuous percent inhibition value (RMSE = 1.157, PCC = 0.743, R^2 = 0.535) [3]. Compounds submitted as PubChem identifiers or SDF files [7] are screened against a 229-kinase panel, and results are returned on one interactive page: an affinity heatmap, two selectivity indices (SI_mean, SI_worst), promiscuity/specificity radar plots, optional AutoDock Vina docking with a 3D viewer [5], and ADMET profiling [6].

In a case study of three FDA-approved ATP-competitive inhibitors absent from the training data, the platform recovered their known profiles: brigatinib gave a sharp, spike-like specificity profile toward ALK (SI_mean = 4.6934), whereas ponatinib (1.7903) and sunitinib (0.9928) were broader, and the docking poses matched their reported Type I and Type II binding modes. Validation against DrugBank sets showed SI_mean shifted upward for approved on-target pairs (n = 422; Wilcoxon $P = 2.48 \times 10^{-9}$), and DeepKinome ranked approved targets above AutoDock Vina. The server is freely available at https://str.kribb.re.kr/deepkinome.

Keywords kinase inhibitor, deep learning, binding affinity prediction, selectivity profiling, drug discovery

Acknowledgments The authors thank members of KRIBB and Gachon University Gil Medical Center for their support and helpful discussions. This work was supported by the Korea Bio Data Station (K-BDS) with computing resources including technical support (KBDSC-2024-KBDS-0066, KBDSC-2025-KBDS-0069, and KBDSC-2025-KBDS-0119 to SN).

References

[1] Manning, G., Whyte, D. B., Martinez, R., et al., Science, 298, 1912 (2002).

[2] Roskoski, R., Pharmacol. Res., 200, 107059 (2024).

[3] Lee, Y., Eun, J., Lee, J., & Nam, S., Front. Mol. Biosci., 12, 1698891 (2025).

[4] Eun, J., Lee, Y., Yang, S., Choi, D., Na, H., Cho, H., Nam, S., & Lee, J., Nucleic Acids Res., 54, W246 (2026).

[5] Trott, O., & Olson, A. J., J. Comput. Chem., 31, 455 (2010).

[6] Swanson, K., Walther, P., Leitz, J., et al., Bioinformatics, 40, btae416 (2024).

[7] Kim, S., Chen, J., Cheng, T., et al., Nucleic Acids Res., 53, D1516 (2025).

pH-dependent membrane insertion and folding of the Caveolin-3-derived peptide Cav3(7–26): an all-atom molecular dynamics study

Seunghoon Yang[1, 2], Youngbeom Cho[1], Ji-Hun Kim[3*], and Jinhyuk Lee[1, 2*]

[1]*Bio-design Editing Research Center, Korea Research Institute of Bioscience and Biotechnology, Daejeon*

[2]*Department of Bioinformatics, KRIBB School of Bioscience, University of Science and Technology, Daejeon*

[3]*Department of Manufacturing Pharmacy, College of Pharmacy, Chungbuk National University, Cheongju*

Caveolin-3 (Cav3) is a muscle-specific scaffolding protein of caveolae whose flexible N-terminal region is intrinsically disordered in solution yet undergoes a pH-dependent conformational switch at membrane-mimetic interfaces [1, 2]. Circular dichroism and NMR show that acidification promotes α-helix formation in the Cav3(7–26) peptide, most strongly at anionic membrane surfaces, but ensemble spectroscopy cannot resolve the time-ordered, residue-level pathway by which the peptide approaches, inserts into, and folds within the bilayer, nor which residues initiate the transition. To obtain this atomic-resolution mechanism, we performed all-atom molecular dynamics (MD) simulations.

Cav3(7–26) was placed at a mixed DMPC/LPPG bilayer interface and simulated for ~10 μs each under fixed protonation states approximating pH 3 (folding) and pH 7 (control) using GROMACS with the CHARMM36m force field [3–5]. At pH 3 the peptide followed an ordered, partly overlapping insertion-and-folding pathway: N-terminal residues made first interfacial contact (~0.8 μs), a short helix was seeded (~1.8 μs), and the peptide settled into a stable 11–17 α-helix buried beneath the lipid phosphates (~6.5–10 μs; modal helix content ~35%). An amphipathic hydrophobic face (Leu9, Ile13, Val14, Ile17) led insertion, with N-terminal residues initiating contact and central residues providing the deepest, most persistent anchor (deepest ~6.5 Å from the bilayer center). At pH 7 the peptide remained disordered in solution (~0% helix), matching the neutral-pH random-coil signature.

To test the role of the flexible termini, the truncation Cav3(10–24), lacking N-terminal 7–9 and C-terminal 25–26, was simulated under the same pH 3 protocol. It formed no 11–17 helix (~0% helix content) and failed to insert (deepest ~19.3 Å, short of the ~17.3 Å bilayer half-thickness), with the deepest position shifting from the helix core to the truncated terminus. This confirms that the terminal residues are essential for the pH-dependent insertion-and-folding transition, consistent with the reduced helical CD of the truncated peptide. Together, the simulations provide a residue-level mechanistic model that unifies the spectroscopic observations and suggest that local acidification, such as lactic-acid accumulation during intense muscle activity or ischemia, could modulate the conformational ensemble of the Cav3 N terminus.

[References]

[1] J.H. Kim, J.P. Schlebach, Z. Lu, D. Peng, K.C. Reasoner, and C.R. Sanders *Biophysical Journal*, **110**, 2475, 2016.

[2] R.G. Parton and M.A. del Pozo *Nature Reviews Molecular Cell Biology*, **14**, 98, 2013.

[3] S. Jo, T. Kim, V.G. Iyer, and W. Im *Journal of Computational Chemistry*, **29**, 1859, 2008.

[4] M.J. Abraham, T. Murtola, R. Schulz, S. Páll, J.C. Smith, B. Hess, and E. Lindahl *SoftwareX*, **1-2**, 19, 2015.

[5] J. Huang, S. Rauscher, G. Nawrocki, T. Ran, M. Feig, B.L. de Groot, H. Grubmüller, and A.D. MacKerell Jr. *Nature Methods*, **14**, 71, 2017.

[6] W. Kabsch and C. Sander *Biopolymers*, **22**, 2577, 1983.

[Key words] Caveolin-3, molecular dynamics, membrane insertion, pH-dependent folding, amphipathic helx

Virtual Screening of Covalent Inhibitors Targeting PNPLA3-I148M

Aejin Kim,[1,2], and Jinhyuk Lee[1,2*]

[1] Bio-design Editing Research Center, Korea Research Institute of Bioscience and Biotechnology (KRIBB), Daejeon 34141, Republic of Korea

[2] School of Food Science & Biotechnology, Kyungpook National University, Daegu 41566, Republic of Korea

The PNPLA3 I148M variant is a major genetic risk factor for metabolic dysfunction-associated steatotic liver disease (MASLD) and accumulates on the lipid droplet surface due to reduced ubiquitination and proteasomal degradation [1]. PF-07853578 has been reported to covalently bind to the catalytic Ser47 residue, promoting the dissociation of PNPLA3 from lipid droplets and subsequent protein degradation [2]. In this study, we aimed to identify novel covalent inhibitor candidates by considering both Ser47 and the local environment surrounding the mutation-specific Met148 residue.

WT and I148M receptor models were constructed from the AlphaFold-predicted human PNPLA3 structure (UniProt Q9NST1). In 1,200 ns MD simulations, the global Cα RMSD was 0.48 Å, while the residue 148–Ser47 OG distance increased from 4.41 Å in WT to 5.27 Å in I148M, indicating a localized active-site difference. Stepwise virtual screening of 24,959 compounds from PF-07853578-based PubChem, amine-ring-expanded, and REINVENT4 de novo libraries yielded 551 candidates for AutoDock4 Flexible Side Chain covalent docking [3] and WT/I148M selectivity assessment. The top-ranked candidate showed an adduct interaction energy of −9.66 kcal/mol with complete pose and energy convergence but dissociated from the catalytic pocket during 100 ns non-covalent MD (ligand RMSD, 12.47 Å; COM displacement, 10.37 Å). In contrast, PF-07853578 remained stable (2.04 Å; 1.56 Å, respectively), while additional top-ranked candidates are currently undergoing MD validation.

This study established an integrated PNPLA3-I148M-targeted virtual screening workflow combining compound filtering, covalent docking, and MD-based validation. The results obtained to date suggest that a high docking score alone does not ensure dynamic binding stability and that MD evaluation incorporating both reactive geometry toward Ser47 and binding stability around Met148 is important for prioritizing candidate compounds.

Keywords PNPLA3-I148M, covalent docking, flexible side chain method, molecular dynamics, Ser47, virtual screening

References

[1] Basu Ray, S., *Adipocyte*, 8, 201–208 (2019).

[2] Pfizer Inc., WO2024084360A1 (2024).

[3] Bianco, G., Forli, S., Goodsell, D. S., Olson, A. J., *Protein Sci.*, 25, 295–301 (2016).

Computational modeling of the AAVX–AAVR complex from Cryo-EM density map

Hongyu Quan[1, †], Seung-Hyun Kim[2, 3, †], Min Kim[2, 3, †], Songyee Jang[4, 5], Jae-Eun Kwon[2, 3], Ok-Seon Kwon[2, 3], Seung Pil Jang[2, 3], Jiwon Ahn[2], Youngbeom Cho[1, 6], Ah-Jun Lee[2], Eun-Hyun Ji[2], Kyung-Sook Chung[2, 3, *], and Jinhyuk Lee[1, 6, *]

[1] Bio-design Editing Research Center, KRIBB, Daejeon 34141, Republic of Korea

[2]Center for Gene and Cell Therapy, KRIBB, Daejeon 34141, Republic of Korea

[3]KRIBB School of Advanced Bioconvergence, Korea University of Science & Technology (UST), Daejeon 34113, Republic of Korea

[4] Microbiome Convergence Research Center, KRIBB, Daejeon 34141, Republic of Korea

[5] Core Research Facility & Analysis Center, KRIBB, Daejeon 34141, Republic of Korea

[6] KRIBB School of Bioscience, Korea University of Science and Technology (UST), Daejeon 34141, Republic of Korea

Adeno-associated virus (AAV) is widely utilized in gene therapy due to its efficient transduction, favorable tissue tropism, and low immunogenicity. Despite its growing therapeutic relevance, the structural basis of its interaction with cellular receptors remains incompletely understood.

To elucidate the mechanism of cellular entry and receptor recognition, we determined the cryo-electron microscopy (cryo-EM) structure of the AAV serotype X (AAVX) capsid in the complex with its cellular receptor, receptor A, at a resolution of 2.66 Å. CHARMM was used to derive an energetically optimized structure with maximal density map–to–model correlation., which provided energetically favorable conformations for the complex, guided initial model construction. Subsequent structural refinement was performed using Phenix real-space refinement and manual corrections in Coot. Interaction analysis provided to identify key contact residues involved in receptor engagement.

This high-resolution density map allowed accurate atomic modeling of the AAVX–receptor A complex, revealing detail interface characterization. These structural insights provide a foundation for understanding the unique receptor engagement of AAVX.

Acknowledgments This research was supported by the Korea Research Institute of Bioscience and Biotechnology (KRIBB) Research Initiative Program (KGM1062511), National Research Council of Science & Technology (NST) grant by the Korea government (MSIT) (No. GTL24021-000) and the Bio & Medical Technology Development Program (RS-2024-00508575).

References

[1] Wang, JH., Gessler, D.J., Zhan, W. et al. Adeno-associated virus as a delivery vector for gene therapy of human diseases. Sig Transduct Target Ther 9, 78 (2024).
[2] Punjani, A., Rubinstein, J., Fleet, D. et al. cryoSPARC: algorithms for rapid unsupervised cryo-EM structure determination. Nat Methods 14, 290–296 (2017).
[3] B. R. Brooks, R. E. Bruccoleri, B. D. Olafson, D. J. States, S. Swaminathan, and M. Karplus: CHARMM: A Program for Macromolecular Energy, Minimization, and Dynamics Calculations, J. Comp. Chem. 4, 187-217 (1983)
[4] PHENIX: a comprehensive Python-based system for macromolecular structure solution. P.D. Adams, P.V. Afonine, G. Bunkoczi, V.B. Chen, I.W. Davis, N. Echols, J.J. Headd, L.W. Hung, G.J. Kapral, R.W. Grosse-Kunstleve, A.J. McCoy, N.W. Moriarty, R. Oeffner, R.J. Read, D.C. Richardson, J.S. Richardson, T.C. Terwilliger, and P.H. Zwart. Acta Cryst. D66, 213-221 (2010).
[5] Emsley P, Lohkamp B, Scott WG, Cowtan K. Features and development of Coot. Acta Crystallogr D Biol Crystallogr. 2010 Apr;66(Pt 4):486-501.

The Intelligent Frontier: Synergizing HPC, AI and Quantum

Korea Supercomputing Conference 2026

KSC2026

2026년 9월 8일(화)~9일(수) | 스위스 그랜드호텔 컨벤션홀(4F)

초고성능 컴퓨팅의 융합을 통해 AI 시대의 과학기술을 이끌어 갑니다.
KSC 2026에 여러분을 초대합니다.

KEYNOTE SPEECH

September 08(THU)

Keynote 1

데이터센터 플래시의 재정의 - AI 시대의 낸드, SSD, 그리고 컨트롤러의 미래

남이현 대표
파두 (FADU)

September 08(THU)

Keynote 2

Quantum Computing Hype vs. Reality

김성혁 상무
LG전자

PROGRAM

DAY 1 | September 08, 2026

- 기조연설 1, 2
- KSC2026 개회식
- Track
  - HPC·AI 인프라 최신 기술 동향 및 국내 대형 시스템 소개 • 2026년 한국계산과학공학회 추계학술대회 • AI for Science: 과학적 발견과 혁신
  - 양자-HPC 하이브리드 컴퓨팅 기술 및 애플리케이션 • 차세대 메모리·가속 컴퓨팅 기술과 클라우드 운영 혁신

DAY 2 | September 09, 2026

- Track
  - HPC 활용을 위한 대규모 데이터 처리 기술 워크숍 · HPC 수치모의실험 전문학 워크숍 · Quantum Intelligence: 양자-AI 융합과 신약 바이오 혁신
  - 국가슈퍼컴퓨터 6호기 '한강' 및 시범·공식서비스(혁신지원사업) 설명회 · HPC 활용 산업 기술 워크숍 · 기상 기후 분야 초고성능컴퓨팅 활용고도화 워크숍
  - Bio-HPC & AI: 차세대 제약 바이오 혁신 · 양자-고전 하이브리드 계산 방법론 및 적용 · 한국초고성능 컴퓨팅포럼기술 교류회

주최 KISTI 한국과학기술정보연구원 | 주관 국가슈퍼컴퓨팅본부 | KSF 한국초고성능컴퓨팅포럼 | KSC4 한국계산과학공학회 | 후원 과학기술정보통신부